Polymer Bulletin (2023) 80:5433–5446
https://doi.org/10.1007/s00289-022-04329-5

ORIGINAL PAPER

Electrical and thermal characterizations of synthesized composite films based on polyethylene oxide (PEO) doped by aluminium chloride ($AlCl_3$)

A. B. Migdadi[1] · Ahmad A. Ahmad[1] · Ahmad M. Alsaad[1] · Qais M. Al-Bataineh[3] · Ahmad Telfah[2,3]

Received: 26 January 2022 / Revised: 24 March 2022 / Accepted: 9 June 2022 /
Published online: 29 June 2022

Abstract

Polymer electrolytes based on poly(ethylene oxide)-aluminium chloride (PEO-$AlCl_3$) are synthesized by the casting method. The crystal structure, chemical bonding, thermal, and electrical properties are investigated and correlated. Particularly, the interplay between the electrical conductivity, crystallinity, and thermal properties of the nanocomposite thin films is tested. Incorporating of suitable amounts of $AlCl_3$ into PEO thin films reduces the crystallinity degree and the crystallite size of the resulting nanocomposite thin films. The measured FTIR profiles confirm the complexation between Al^{-3} ions and the ether oxygen of the PEO host polymer. Furthermore, the melting temperature and melting enthalpy are significantly reduced by adding the ionic salt into the PEO thin films. Electrical characterization of the PEO-$AlCl_3$ thin films is performed using the four-point probe. The electrical conductivity, the conductivity maps, and activation energy of PEO-$AlCl_3$ nanocomposite films are investigated to elucidate the effect of the complexation between Al^{-3} ions and the ether oxygen of the host polymer. The room temperature conductivity of the pure PEO thin films is measured to be 1.67×10^{-4} S/cm. The highest value of the conductivity is attained for PEO doped by 5 wt% of $AlCl_3$. Moreover, electrical conductivity of all PEO-$AlCl_3$ nanocomposite thin films is found to enhance with increasing temperature. The optimized conductivity of PEO nanocomposite films doped by 20 wt% $AlCl_3$ at 328 K is attained. The enhancement of physical and chemical properties of PEO-$AlCl_3$ may pave the way to manufacture polymer nanocomposite films that could be potential candidates to fabricate high-efficiency photovoltaic devices.

Keywords Polyethylene oxide (PEO) · Sheet resistance · Electrical conductivity · Conductivity maps · Aluminium chloride ($AlCl_3$) · Four-point probe technique

✉ Ahmad M. Alsaad
alsaad11@just.edu.jo; amalsaad@unomaha.edu

Extended author information available on the last page of the article

Introduction

Polymer electrolytes have attracted significant attention owing to their controllable physical and chemical properties. This class of polymers has been utilized in several applications and in developing photovoltaic devices, energy storage, sensors, and actuators [1]. Among these, polyethylene oxide (PEO) is considered one of the most critical electrolyte synthetic polymers due to its good physicochemical properties as compared to other polyelectrolytes [2–4]. Moreover, it has an excellent ability to dissociate ions and dissolve ionic salts even at very high salt concentrations [5]. The ability to dissolve ionic salts takes place via the association of the cations with oxygen atoms in the PEO chains [6]. PEO has a high solubility in organic solvents making it easy to fabricate in the form of solid films [7, 8]. In addition, PEO is a semiconductor material with low electrical conductivity. It is the most promising material for developing polymer batteries [9]. PEO has been used widely as a host matrix material for Li-ion polymer batteries [10].

Furthermore, PEO has a semicrystalline nature at room temperature. Therefore, the crystalline phases hinder ion conduction by blocking charge carriers in the internal boundaries of the PEO chain leading to a limiting conductivity performance [8, 11]. In contrast, the amorphous phase is distinguished by a highly flexible backbone that contributes to boosting the ionic conductivity through greater ionic diffusivity [12]. Likewise, the ionic conductivity and charge diffuse are related to the segmental motion of the polymer chains. Improving the segmental motion enhances charge carriers mobility within the amorphous phase of the polymer matrix [13, 14]. In this prospective, the electrical conductivity could be enhanced by several factors such as temperature and by doping the polymer with suitable inorganic ionic salt, especially alkali metal salts [15]. Aluminium ions (Al^{+3}) could be added to the polymer matrix as intense ions using $AlCl_3$ or other ionic forms.

The DC electrical conductivity could, however, be measured using a different method. One of the most common straightforward modern methods is the four-point probe technique that can measure the volume conductivity of the samples by considering the grain boundary conductivity [16]. The four-point probe technique could give an unequivocal value of the total conductivity [17].

In the present work, PEO-$AlCl_3$ composite films with different ionic salt contents of $AlCl_3$ are prepared. The main aim of this study is to investigate the influence of the ionic salt concentration and the temperature (298–328 K) on electrical conductivity properties. Particularly, their influence on the ion transport properties, conductivity mapping, and activation energy will be studied in detail. To the best of our knowledge, no previous studies have been conducted to investigate the electrical conductivity and conductivity mapping of PEO composite films doped by $AlCl_3$ ions.

Materials and methods

Synthesis of PEO-$AlCl_3$ nanocomposites films

Polyethylene oxide (PEO) with M_W of 300.000 g/mol, aluminum chloride ($AlCl_3$) with M_W of 133.34 g/mol, and absolute methanol (CH_3OH) were purchased from Sigma-Aldrich. A stock solution of PEO was prepared by dissolving 1.0 g PEO in 100 mL of methanol. The solution was stirred at about 45 °C and left for the next day to get a homogeneous solution. The composite solutions of PEO-$AlCl_3$ with different amounts of $AlCl_3$ (wt% = 0%, 2.5%, 5%, 10%, and 20%) are prepared by adding suitable amounts of $AlCl_3$ directly into 20 mL of PEO solution. The mixture is then exposed to ultrasonic Probe for 5 min under continuous magnetic string until the mixture becomes thoroughly homogenous. The PEO-$AlCl_3$ composite thin films are then deposited on the glass substrates by casting technique. The thin films are produced by letting the solvent dry for 24 h at room temperature.

Characterizations techniques

Powder X-ray diffraction (XRD, Malvern Panalytical Ltd, Malvern, UK) and Fourier transform infrared spectroscopy (FTIR, Bruker VERTEX 80/80v Vacuum FTIR Spectrometers) were used to examine the crystal and chemical structure of PEO-$AlCl_3$ nanocomposite films. Differential scanning calorimetry (DSC 204F1, Netzsch-Proteus) was used to measure the heat flow of the PEO-$AlCl_3$ nanocomposite films. Two milligrams of each sample was heated with a heating rate 10 °C / min under a nitrogen flow. A four-point probe (Microworld Inc.) coupled to a high-resolution multimeter was used to investigate the electrical properties of all samples (Keithley 2450 source meter).

Results and discussions

Crystal and chemical structure

Figure 1 displays the XRD patterns of pure PEO and PEO-$AlCl_3$ nanocomposite films at 2θ ranging from 10 to 50°. The main sharp peaks appeared at the angular positions of 19° and 23° belong to the PEO confirming the crystalline nature of PEO. The first peak at 19° corresponds to the interchain distance (4.67 Å), and the second peak at 23° corresponds to chain fold distance (3.83 Å). No peaks belonging to $AlCl_3$ in the XRD patterns are detected indicating the total dissolution of salt within the polymer matrix. The sharp peaks of PEO exhibit flattening and broadening with low intensity as contents of $AlCl_3$ are increased suggesting that the amorphous phase is dominant in PEO-$AlCl_3$ nanocomposite films [18]. This may be attributed to the disruption of the PEO structure due to interaction between the polymer chains and ionic salt that reduces the intermolecular interaction between

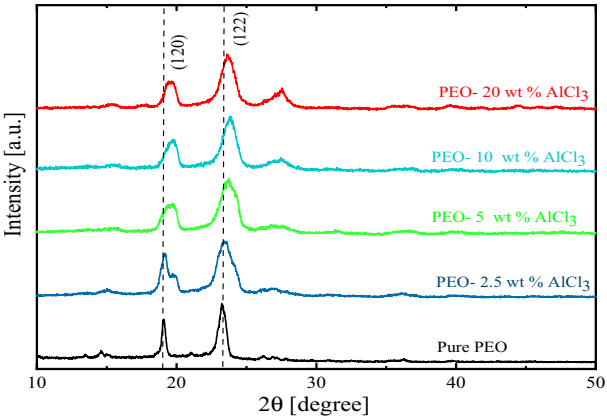

Fig. 1 The XRD patterns of PEO-$AlCl_3$ nanocomposite films with various concentrations of $AlCl_3$

molecules [19]. In other words, the Al^{+3} ions restrain the packing of PEO molecules due to the coordination bonds between ether O atoms (C–O–C group) of PEO and Al^{+3} ions [20]. Remarkably, the dominant amorphous phase is distinguished by a highly flexible backbone that contributes to boosting the ionic conductivity through greater ionic diffusivity [12].

Moreover, when increasing the ionic concentration by more than 10 wt.%, a broad peak with low intensity located at $2\theta = 27°$ starts appearing and becomes more evident especially for PEO-$AlCl_3$ 20 wt% thin films. This result suggests an increase in the crystallinity compared to the PEO films with a low salt concentration. To elucidate this effect, the degree of crystallinity (X_c) of PEO-$AlCl_3$ can be estimated by $X_c = A_{\text{cres}}/A_{\text{total}} \times 100\%$ [21]. The (X_c) of pure PEO is 32.6%. Addition of 5 wt% of $AlCl_3$ into the polymer electrolyte reduces the crystallinity to 27.4%. It was noticed that the addition of 20 wt% of ionic salt into the PEO films led to an increase in the crystallinity to become 29.9%. Similar behavior of crystallinity has been reported in a previous work [22].

The key mechanical and elastic parameters such as crystallite size ($D = \lambda k/\beta \cos\theta$), microstrain ($\varepsilon = \beta \cot\theta/4$), dislocations density $\left(\delta = 1/D^2\right)$, crystallite density $\left(N = t/D^3\right)$, total internal stress ($\sigma = E * \varepsilon$), and strain energy density $\left(E_d = E\varepsilon^2/2\right)$ are also estimated for all investigated PEO-$AlCl_3$ nanocomposite films. The parameters used are λ, the wavelength of the X-ray ($\lambda = 0.154184$ nm), β is the full width at half maximum in radians, θ is Bragg's angle, and k is Scherrer constant (0.94), E is Young's modulus, and t is the film thickness [23–29]. The obtained values are summarized in Table 1.

The crystallite size of PEO-$AlCl_3$ exhibits a significant decrease. It decreases from 18.6 to 7.2 nm upon introducing 5 wt% of $AlCl_3$ into PEO matrix. Consequently, both dislocations and crystallite density of the nanocomposite thin films increase. Furthermore, the dislocations density increases indicating more free spaces available and less crystallization and thus enhancing the charge carriers' mobility within the polymer matrix. These results are in good agreement with those

Table 1 The structure parameters of PEO composite films with different contents of $AlCl_3$

Content [wt.%]	X_c%	D [nm]	$\epsilon(10^{-2})$	δ* (10^{11}) [lines/cm^2]	(N)*10^{13} [crys. / cm^2]	$\sigma * 10^{-1}$[GPa]	$E_d * 10^6$[J.m^{-3}]
0%	32.6	18.6	1.16	0.28	0.77	0.65	2.10
2.5%	29.6	9.8	2.25	1.03	5.26	1.24	7.09
5%	27.3	7.2	2.71	1.94	13.5	1.49	18.3
10%	29.8	8.1	2.39	1.54	9.59	1.31	17.6
20%	29.9	8.5	2.28	1.37	8.05	1.25	13.6

The significance of the parameters indicated in bold is revealed by indicating the significant effect of inserting different concentrations (wt.%) of $AlCl_3$ on key structural parameters of PEO thin films

previously reported [30, 31]. The microstrain has also been noticed to exhibit a significant increase different amounts of $AlCl_3$ which are introduced in the polymer matrix. This may be attributed to the electrostatic interactions between the polymer chains and ionic salt that increase the strain energy in the PEO-$AlCl_3$ composite films and produce deformation in the structure. As a result, the di-electricity properties of the material are enhanced. The total internal stress and strain energy density of pure PEO film are estimated to be 0.65×10^{-1} GPa and 2.1×10^6j.m^{-3}, respectively. Both increase due to the injecting of various amounts of $AlCl_3$ into the PEO matrix as shown in Table 1.

Figure 2 shows the FTIR spectra of pure PEO and PEO-$AlCl_3$ composite films incorporated with various concentrations of $AlCl_3$. Generally, there is no significant effect on the bonds of PEO upon the injection of different amounts of $AlCl_3$ into the PEO matrix. A small peak at about 526 cm^{-1} is assigned to $-CH_2$ stretching. The vibrational bands that are perceived between 700 and 1000 cm^{-1} are assigned to the C–H bending vibrations. The vibrational bands between 1000 and 1400 cm^{-1} correspond to the C–O–C stretching vibrations. In addition, $-CH_2$ bending vibration

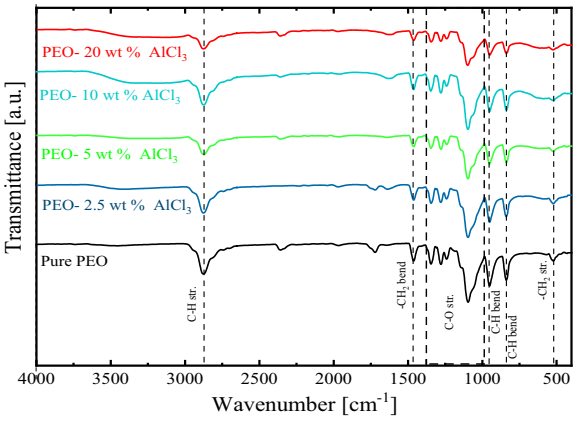

Fig. 2 The FTIR spectra of PEO-$AlCl_3$ composite films with various concentrations of $AlCl_3$

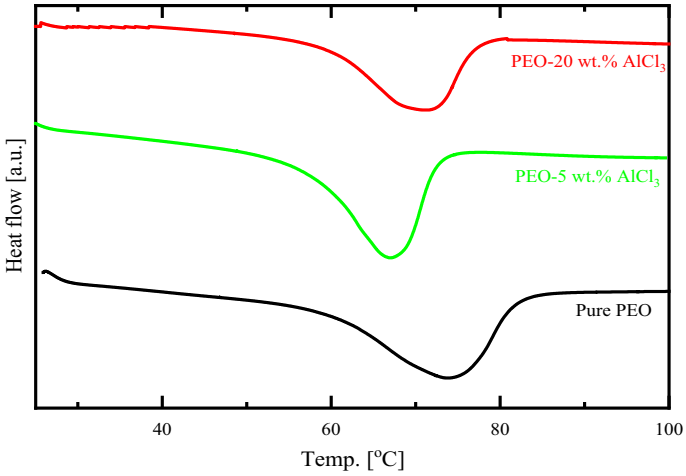

Fig. 3 The DSC curves of PEO-$AlCl_3$ nanocomposite films

Table 2 The DSC parameters of PEO-$AlCl_3$ nanocomposite films

Content [wt%]	T_0 [°C]	T_e [°C]	T_m [°C]	ΔH_p [J/g]	X_c [%]
0%	61.7	81.3	74	116.6	57.4
5%	59	72.2	67	107.8	53.1
20%	60.4	76.5	70.9	92.14	45.4

appeared at 1464 cm^{-1} [32]. The symmetric and asymmetric C–H stretching vibrations are observed at 2880 cm^{-1} that exhibit smaller width and intensity as $AlCl_3$ is introduced in the PEO matrix. The decrease in the width and intensity may be attributed to the high electronegativity of Al^{-3} ions as compared with the PEO molecules [33]. Furthermore, it looks there is a tiny intensity vibration band within (3300 cm^{-1} to 3660 cm^{-1}) spectral range associated with the O–H band (hydroxyl band). This band becomes more apparent at high concentrations of ionic salt. This result may confirm the complexation that occurs between Al^{-3} ions and the ether oxygen of the host polymer [32, 34].

Differential scanning calorimeter (DSC)

DSC analysis is considered as one of the most appropriate methods for analyzing the thermal properties of semicrystalline polymers. Figure 3 shows the DSC curves of PEO-$AlCl_3$ composite films. Each DSC curve demonstrates an endothermic peak due to the melting temperature (T_m) of the polymer electrolytes. The endothermic peak occurs due to the absorption of thermal energy by the sample. All the DSC parameters, including onset temperature (T_0), end temperature T_e, melting temperature (T_m), and fusion enthalpy (ΔH_m), are represented in Table 2. The peak value represents the melting temperature (T_m). The T_m is found to be 74 °C,

67 °C, and 71 °C for pure PEO, PEO-5 wt% $AlCl_3$, and PEO-20 wt% $AlCl_3$, respectively. Clearly, introducing $AlCl_3$ into PEO films results in a reduction of the melting temperature indicating the relaxation of the polymer chains and more flexibility is inherited. Moreover, the fusion enthalpy $\left(\Delta H_m\right)$ can be determined from the area of endothermic peak. It exhibits a significant reduction upon the incorporation of $AlCl_3$ into PEO matrix. The values of ΔH_m are found to be 116.6 J/g, 107.8 J/g, and 92.14 J/g for pure PEO, PEO-5 wt. % $AlCl_3$, and PEO-20 wt.% $AlCl_3$, respectively. The decrease in the melting temperature and the fusion enthalpy may be attributed to a discontinuity in the PEO chains as well as a reduction in the interaction forces between the molecules within the PEO matrix as the ionic salt is added to the polymer matrix [35]. In other words, the Al^{+3} and Cl^{-2} ions may work to cut out the packing of the PEO backbone and enhance the mobility of segment motion, subsequently reducing the crystallinity and improving the ionic conductivity of the PEO [36, 37]. The obtained results of melting temperature and the fusion enthalpy agree with the previous studies [37, 38].

Moreover, the crystallinity $\left(X_c\right)$ of samples can also be estimated as [39],

$$X_c = \frac{\Delta H_c}{\Delta H_p} * 100\% \tag{1}$$

The ΔH_p is the fusion enthalpy of pure PEO of 100% crystallinity (203 J/g), and ΔH_c is the fusion enthalpy of the prepared films. The pure PEO film exhibits a higher value of crystallinity calculated to be about 57.4%. However, the crystallinity decreases to 45% for PEO-20 wt% $AlCl_3$. The crystallinity obtained from XRD or DSC follows the same behavior. We observe that the DSC scan speed may affect the fusion enthalpy and melting temperature and subsequently impacting the crystallinity [38]. The obtained results from the DSC data demonstrate a correlation between the ionic salt and each fusion enthalpy, the crystallinity of the films, and the ionic conductivity.

Electrical conductivity and sheet resistance

The variation in the sheet resistance and the electrical conductivity of PEO-$AlCl_3$ nanocomposite films was plotted as a function of concentrations of $AlCl_3$ at different temperatures (298 K, 308 K, 318 K, 328 K), as shown in Fig. 4a, b. The electrical conductivity (σ) of films is related directly to the resistivity (ρ), sheet resistance $\left(R_s\right)$, and thickness of the film (t) by $\sigma = 1/\rho$ and $\rho = tR_s$, and the thickness of films was estimated to be about one μm [40, 41].

Obviously, the electrical conductivity exhibits a reverse behavior to that of the sheet resistance as shown in Fig. 4. The effect of $AlCl_3$ content and temperatures on the conductivity is illustrated in Fig. 4.

At room temperatures condition, R_s of pure PEO thin films is calculated to be 5.52×10^7 Ω/sq. It decreases to 3.9×10^7 Ω/sq for PEO-$AlCl_3$ containing 5 wt% of $AlCl_3$. The σ parameter of pure PEO thin films is found to be 1.67×10^{-4} S/cm. It increases to a maximum value of 5.1×10^{-4} S/cm for PEO doped with 5 wt% of $AlCl_3$. Remarkably, PEO films doped by 5 wt% of $AlCl_3$ have the smallest degree

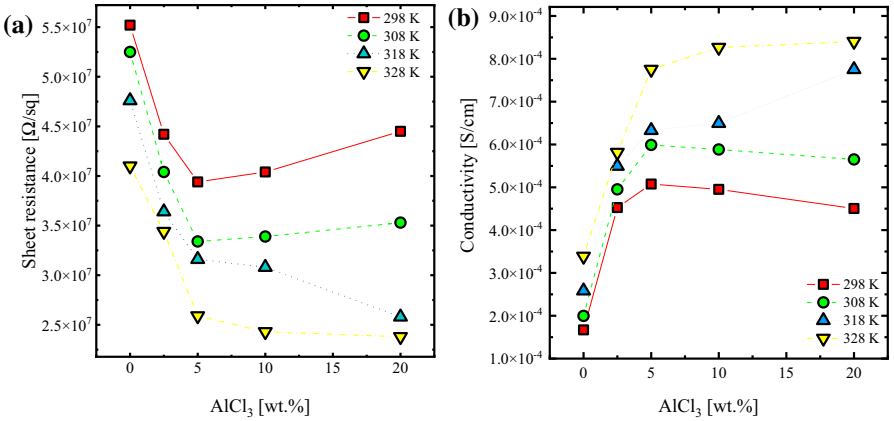

Fig. 4 **a** The sheet resistance and **b** electrical conductivity of the PEO-$AlCl_3$ composite films as a function of $AlCl_3$ [wt.%]

of crystallinity as presented in Table 1. Increasing the conductivity with increasing the ionic concentration (Al^{+3}) in the polymer matrix is attributed to the increase of the concentration and mobility of charge carriers. This is caused by the segmental motion of Al^{+3} through the amorphous nature of the polymer chains. It is worth mentioning that the DC conductivity of the dielectric materials is related directly to carriers concentration and carriers mobility by $\sigma = en_e\mu_e$ [42]. The reduction in the cohesion force of polymer chains is accountable for facilitating the segmental motion and thus enhancing charge carriers mobility within the polymer matrix [13]. Additionally, bridging the gaps between the localized states through the Al^{+3} ions may improve the electrical conductivity [43].

As can be seen from Fig. 4, conductivity exhibits a slight reduction upon introducing 10 wt% and 20 wt% of $AlCl_3$. This could be attributed to an accumulation of Al^{+3} ions that restricts the carriers mobility and increases the crystallinity of the polymeric matrix in consistent with the XRD findings. On the other hand, strong electrostatic interactions between Al^{+3} ions and the negative charges of the ether oxygen atoms of the PEO chain may reduce the dipole moment and the dielectric polarization. Consequently, it hinders segmental motion and carriers mobility [42].

Furthermore, the electrical conductivity of all PEO-$AlCl_3$ nanocomposite thin films is enhanced as the temperature is increased as shown in Fig. 4b. This enhancement is due to Al^{+3} ions' thermal activation energy that makes them transfer to another coordinating site [1]. Moreover, increasing the temperature leads to incremental segment motion against the cohesive force depending on the energy of segment vibrations [44]. The overall behavior of the conductivity at 298 K and 308 K is similar, and the highest value is obtained for PEO-$AlCl_3$ (5 wt%). However, it exhibits a significant change at 318 K and 328 K and the highest value is obtained for PEO-$AlCl_3$ (20 wt%). This could be interpreted in terms of increasing the thermal energy that increases the available volume around the polymer chains leading to overcoming constraints of ions accumulation at high doping levels and enhancing

mobility [1, 45]. Interestingly, the PEO-20 wt% $AlCl_3$ nanocomposite thin films at 328 K exhibit the highest possible value of conductivity $\left(8.4 \times 10^{-4}\ \text{S/cm}\right)$ and smallest value of sheet resistance ($2.3{\times}10^7$ Ω/sq). The activation energy (E_a) of the PEO-$AlCl_3$ nanocomposite films has been estimated by Arrhenius equation; $\sigma = \sigma_0 \exp\left(-E_a/K_B T\right)$, where σ_0 is the pre-exponential factor, T is the temperature [K], and K_B is the Boltzmann constant [4]. It expresses the required energy of ions hops between the localized states and the energy of defects formation [46]. The E_a parameter is calculated from the slopes of ln (σ) versus 1000/T(K) for the PEO-$AlCl_3$ nanocomposite films containing various contents of $AlCl_3$ (Fig. 5a).

Figure 5b shows the variation of activation energy as a function of $AlCl_3$ contents for PEO films. Obviously, adding various concentrations of $AlCl_3$ into PEO films reduces the activation energy and thus an electrical conductivity enhancement. The highest value of E_a is attained for pure PEO films indicating that these films require the highest energy for hopping between the localized sites. In contrast, the smallest value (about 0.07 eV) is obtained for PEO-$AlCl_3$ (2.5 wt%). Thus this film exhibits an increase in ions' mobility through the dominant amorphous nature of the polymer matrix [3]. Adding more content of $AlCl_3$ ions into the PEO films increases the concentration of charge carriers that seemingly need more activation energy for hopping between the localized states. This explains the high values of the activation energy for PEO-$AlCl_3$ nanocomposites containing 5 wt%, 10 wt%, and 20 wt%.

Figure 6a–c shows the conductivity map of pure PEO and PEO-$AlCl_3$ (20 wt%) nanocomposite films at room temperate and at 328 K. It indicates the variations of the conductivity over multiple locations in the films. Several factors influence the conductivity distribution such as ions concentrations Al^{+3}, the grain size related to the growth process, local adsorption of environmental contaminants and wrinkles or cracks in the surface [47].

The conductivity values of pure PEO film at 298 K range from 2.7×10^{-4} to 4.7×10^{-4} S/cm across the film. Incorporation of 20 wt% of $AlCl_3$ into the polymer

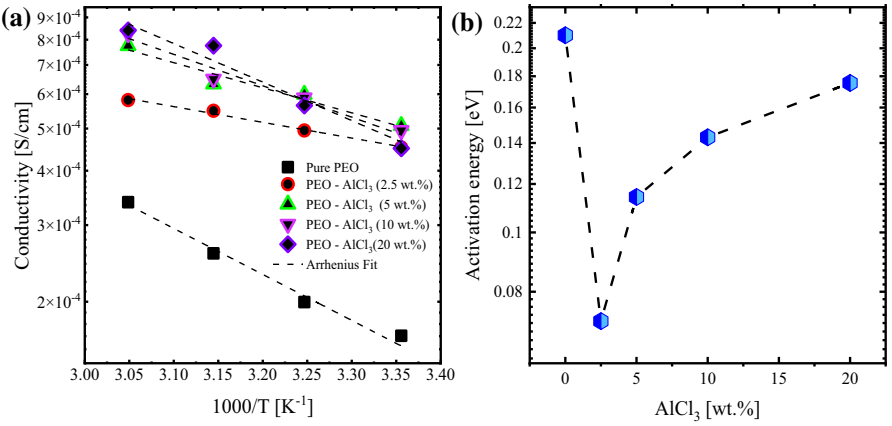

Fig. 5 **a** The electrical conductivity of PEO-$AlCl_3$ composite films as a function of 1000/T [$K.^{-1}$] and **b** activation energy deduced from conductivity fitted to Arrhenius law in the 298–328 K temperature range

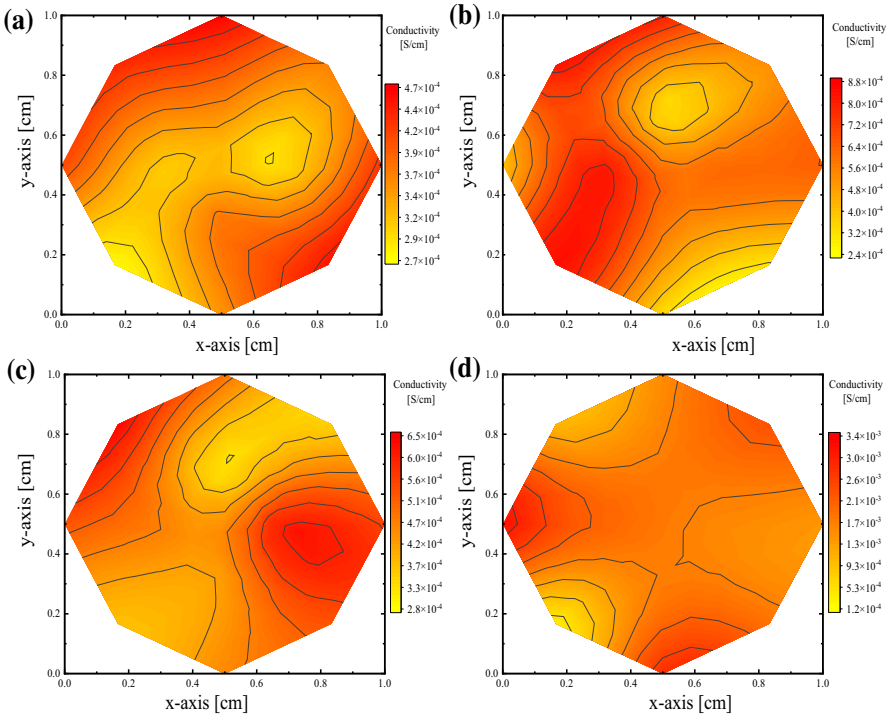

Fig. 6 The conductivity maps **a** PEO film at room temperature (298 K), **b** PEO film at 328 K, **c** PEO-$AlCl_3$ (20 wt %) at room temperature (298 K) and **d** PEO-$AlCl_3$ (20 wt.%) at 328 K

matrix leads to a change in conductivity distribution from one point to another due to the increased Al^{+3} ions concentrations as demonstrated in Fig. 6a and c. Elevating the temperature to 328 K has a significant impact on the conductivity distribution of pure PEO and PEO-$AlCl_3$ (20 wt%) films that could be attributed to the increasing of the segment motion and enhancing the mobility of charge carriers through the PEO-$AlCl_3$ nanocomposite films as can be clearly seen from Fig. 6c and d. The conductivity values of PEO-$AlCl_3$ (20 wt%) films at 328 K range from 1.2×10^{-4} to 3.4×10^{-3} S/cm.

Conclusions

In summary, polymer electrolytes nanocomposite films (PEO-$AlCl_3$) are synthesized and characterized. The as-prepared thin films exhibit a semicrystalline nature indicating that the crystalline peaks overlap with the amorphous band. Incorporating suitable amounts of $AlCl_3$ into PEO films leads to a reduction in the crystallinity degree of the composite films. The amorphous nature contributes to boosting the ionic conductivity through greater ionic diffusivity. This could be attributed to the enhancing of the segmental motion of the polymer matrix. The crystallite size of pure PEO film is 18.6 nm that decreases depending on the

content of $AlCl_3$ ionic salt in the PEO matrix. In contrast, the microstrain, dislocations density, crystallite density, total internal stress, and strain energy density all increase as the content of $AlCl_3$ is increased in the PEO matrix. This may be attributed to the electrostatic interactions between the polymer chains and ionic salt, consequently, increasing the strain energy in the PEO-$AlCl_3$ composite films and producing deformation in the structure. The significant increase in these parameters results in improving the di-electricity properties of the films.

To elucidate the effect of introducing the ionic salt on the lattice dynamics and vibrational models of the films, FTIR spectra demonstrate no significant effect. However, the O–H band (hydroxyl band) becomes more apparent especially at high concentrations of ionic salt. This result confirms the complexation that occurs between Al^{-3} ions and the ether oxygen of the host polymer.

Analyzing DSC data confirms the relationship between the ionic salt and each fusion enthalpy, the crystallinity of the films, and the ionic conductivity. Adding $AlCl_3$ into PEO films leads to a decrease in the melting temperature, fusion enthalpy, and crystallinity.

The impact of the ionic salt ($AlCl_3$), as well the temperature on the sheet resistance, the electrical conductivity, and the conductivity mapping of PEO-$AlCl_3$ composite films, is investigated and interpreted. The conductivity of pure PEO thin films at room temperature is found to be 1.67×10^{-4} S/cm. It increases to the highest value of about 5.1×10^{-4} S/cm for PEO doped by 5% wt of $AlCl_3$. Furthermore, electrical conductivity of all PEO-$AlCl_3$ composite films is enhanced as the temperature is increased. The PEO composite film doped by 20 wt % of $AlCl_3$ at 328 K exhibits the highest value of conductivity (8.4×10^{-4} S/cm). Moreover, inserting various concentrations of $AlCl_3$ into PEO films reduces the activation energy. Therefore, the concentration of charge carriers is considerably increased.

The conductivity maps of pure PEO film and PEO-$AlCl_3$ composite film doped by 20 wt % at room temperature (298 K) and 328 K exhibit variations of the electrical conductivity depending on the $AlCl_3$ contents. Several factors contribute to the conductivity distribution such as ions concentrations Al^{+3}, the grain size related to the growth process, local adsorption of environmental contaminants and wrinkles or cracks in the surface. The results reported in this work may pave the way to fabricate polymer composite films that could be potential candidates for the fabrication of high-efficiency scaled functional photovoltaic devices.

Acknowledgements The authors would like to acknowledge the deanship of scientific research at Jordan University of Science and Technology for financial, technical, and logistic support. Special acknowledgments are forwarded to Prof. Borhan Albiss and Prof. Mohammad Al-Omari at the department of Physics, Jordan University of Science and Technology, for the access provided for their laboratories.

Author Contributions ABM, AAA, AMA, QMA, AT contributed to conceptualization; ABM, AAA, AMA, QMA, AT contributed to methodology; ABM, AAA, AMA, QMA, AT contributed to investigation**;** ABM, AAA, AMA, QMA, AT contributed to data curation; ABM, AAA, AMA, QMA, AT contributed to formal analysis; ABM, AAA, AMA, QMA, AT contributed to writing-original draft; ABM, AAA, AMA, QMA, AT contributed to writing–review and editing; AAA, AMA contributed to funding acquisition; AAA, AMA contributed to project administration; AAA, AMA contributed to resources; AAA, AMA contributed to supervision; ABM, AAA, AMA, QMA, AT contributed to validation; ABM,

AAA, AMA, QMA, AT contributed to visualization. All authors have read and agreed to the published version of the manuscript.

Funding Jordan University of Science and Technology, 350-2020, Ahmad Alsaad.

Data Availability The data presented in this study are available on request from the corresponding author.

Declarations

Conflict of interest The authors declare no conflict of interest (financial or nonfinancial).

References

1. AL-Akhras MA, Alzoubi SE, Ahmad AA, Ababneh R, Telfah A (2021) Studies of composite films of polyethylene oxide doped with potassium hexachloroplatinate. J Appl Polym Sci 138(5):49757
2. Dhatarwal P, Sengwa RJCC (2020) Dielectric relaxation, Li-ion transport, electrochemical, and structural behaviour of PEO/PVDF/LiClO4/TiO2/PC-based plasticized nanocomposite solid polymer electrolyte films. Compos Commun 17:182–191
3. Telfah A, Abdul-Gader Jafar MM, Jum'h I, Ahmad MJA, Lambert J, Hergenröder R (2018) Identification of relaxation processes in pure polyethylene oxide (PEO) films by the dielectric permittivity and electric modulus formalisms. Polym Adv Technol 29(7):1974–1987
4. Telfah A et al (2021) Dielectric relaxation, XPS and structural studies of polyethylene oxide/iodine complex composite films. Polym Bull 79:1–20
5. Ferloni P, Chiodelli G, Magistris A, Sanesi M (1986) Ion transport and thermal properties of poly (ethylene oxide)-LiClO4 polymer electrolytes. Solid State Ionics 18:265–270
6. Kumar KK, Ravi M, Pavani Y, Bhavani S, Sharma A, Rao VVRN (2011) Investigations on the effect of complexation of NaF salt with polymer blend (PEO/PVP) electrolytes on ionic conductivity and optical energy band gaps. Phys B Condens Matter 406(9):1706–1712
7. Siemann U (2005) Solvent cast technology–a versatile tool for thin film production. Scattering methods and the properties of polymer materials. Springer, pp 114
8. Schönherr H, Frank CW (2003) Ultrathin films of poly (ethylene oxides) on oxidized silicon. 1. Spectroscopic characterization of film structure and crystallization kinetics. Macromolecules 36(4):1188–1198
9. Markus P, Martínez-Tong DE, Papastavrou G, Alegria AJSM (2020) Effect of environmental humidity on the ionic transport of poly (ethylene oxide) thin films, investigated by local dielectric spectroscopy. Soft Matter 16(13):3203–3208
10. Long L, Wang S, Xiao M, Meng Y (2016) Polymer electrolytes for lithium polymer batteries. J Mater Chem A 4(26):10038–10069
11. Money BK, Swenson J (2013) Dynamics of poly (ethylene oxide) around its melting temperature. Macromolecules 46(17):6949–6954
12. Mohamad A et al (2003) Ionic conductivity studies of poly (vinyl alcohol) alkaline solid polymer electrolyte and its use in nickel–zinc cells. Solid State Ionics 156(1–2):171–177
13. Rathika R, Padmaraj O, Suthanthiraraj SAJI (2018) Electrical conductivity and dielectric relaxation behaviour of PEO/PVdF-based solid polymer blend electrolytes for zinc battery applications. Ionics 24(1):243–255
14. Borodin O, Smith GD (2006) Mechanism of ion transport in amorphous poly (ethylene oxide)/LiTFSI from molecular dynamics simulations. Macromolecules 39(4):1620–1629
15. Zhou D, Shanmukaraj D, Tkacheva A, Armand M, Wang GJC (2019) Polymer electrolytes for lithium-based batteries: advances and prospects. Chem 5(9):2326–2352
16. Badwal SPS (1983) Electrical conductivity of Sc 2 O 3-ZrO 2 compositions by 4-probe dc and 2-probe complex impedance techniques. J Mater Sci 18(10):3117–3127

17. Li Q, Thangadurai V (2010) A comparative 2 and 4-probe DC and 2-probe AC electrical conductivity of novel co-doped Ce 0.9−*x*RE*x*Mo 0.1 O 2.1–0.5 x (RE = Y, Sm, Gd; $x = 0.2, 0.3$). J Mater Chem 20(37):7970–7983
18. Reddeppa N, Sharma A, Rao VN, Chen WJME (2013) Preparation and characterization of pure and KBr doped polymer blend (PVC/PEO) electrolyte thin films. Microelectron Eng 112:57–62
19. Nadimicherla R, Kalla R, Muchakayala R, Guo XJSSI (2015) Effects of potassium iodide (KI) on crystallinity, thermal stability, and electrical properties of polymer blend electrolytes (PVC/PEO: KI). Solid State Ionics 278:260–267
20. Klongkan S, Pumchusak JJEA (2015) Effects of nano alumina and plasticizers on morphology, ionic conductivity, thermal and mechanical properties of PEO-LiCF3SO3 solid polymer electrolyte. Electrochim Acta 161:171–176
21. Kumar A, Saikia D, Singh F, Avasthi DK (2005) Ionic conduction in 70 MeV $C5^{+}$ ion-irradiated P (VDF–HFP)–(PC+DEC)–LiCF3SO3 gel polymer electrolyte system. Solid State Ionics 176(17–18):1585–1590
22. Chaurasia SK, Singh RK, Chandra S (2011) Structural and transport studies on polymeric membranes of PEO containing ionic liquid, EMIM-TY: evidence of complexation. Solid State Ionics 183(1):32–39
23. Alsaad A, Ahmad A, Qattan I, Al-Bataineh QM, Albataineh Z (2020) Structural, optoelectrical, linear, and nonlinear optical characterizations of dip-synthesized undoped ZnO and group III elements (B, Al, Ga, and In)-doped ZnO thin films. Crystals 10(4):252
24. Al-Bataineh QM, Alsaad A, Ahmad A, Al-Sawalmih A (2019) Structural, electronic and optical characterization of ZnO thin film-seeded platforms for ZnO nanostructures: sol–gel method versus ab initio calculations. J Electron Mater 48(8):5028–5038
25. Alsaad AM et al (2020) Optical, Structural, and Crystal Defects Characterizations of dip Synthesized (Fe–Ni) co-doped ZnO thin films. Materials 13(7):1737
26. Al-Bataineh QM et al (2020) Synthesis, crystallography, microstructure, crystal defects, optical and optoelectronic properties of ZnO:CeO2 mixed oxide thin films. Photonics 7(4):112
27. Alsaad A et al (2020) Measurement and ab initio investigation of structural, electronic, optical, and mechanical properties of sputtered aluminum nitride thin films. Frontiers in Physics 8:115
28. Ahmad A, Migdadi A, Alsaad A, Al-Bataineh QM, Telfah AJAPA (2021) Optical, structural, and morphological characterizations of synthesized (Cd–Ni) co-doped ZnO thin films. Appl Phys A 127(12):1–12
29. Ahmad AA, Migdadi A, Alsaad AM, Qattan I, Al-Bataineh QM, Telfah AJH (2021) Computational and experimental characterizations of annealed Cu2ZnSnS4 thin films. Heliyon 8:e08683
30. Akl AA, Hassanien A (2015) Microstructure and crystal imperfections of nanosized CdSxSe1−*x* thermally evaporated thin films. Superlattices Microstruct 85:67–81
31. Williamson G, Smallman R (1956) III. Dislocation densities in some annealed and cold-worked metals from measurements on the x-ray debye-scherrer spectrum. Phil Mag 1(1):34–46
32. Ahmed HT, Abdullah OGh (2020) Structural and ionic conductivity characterization of PEO: MC-NH4I proton-conducting polymer blend electrolytes based films. Results Phys 16:102–861
33. Bazaka K, Jacob MV (2017) Effects of iodine doping on optoelectronic and chemical properties of polyterpenol thin films. Nanomaterials 7(1):11
34. Mohan V, Raja V, Sharma A, Rao VN (2006) Ion transport and battery discharge characteristics of polymer electrolyte based on PEO complexed with NaFeF 4 salt. Ionics 12(3):219
35. Sganzerla WG et al (2020) Nanocomposite poly (ethylene oxide) films functionalized with silver nanoparticles synthesized with *Acca sellowiana* extracts. Coll Surf A Physicochem Eng Asp 602:125125
36. Jinisha B, Anilkumar K, Manoj M, Pradeep V, Jayalekshmi SJEA (2017) Development of a novel type of solid polymer electrolyte for solid state lithium battery applications based on lithium enriched poly (ethylene oxide)(PEO)/poly (vinyl pyrrolidone) (PVP) blend polymer. Electrochim Acta 235:210–222
37. Wang H et al (2020) Mechanical property-reinforced PEO/PVDF/LiClO4/SN blend all solid polymer electrolyte for lithium ion batteries. J Electroanal Chem 869:114156
38. da Rosa CG et al (2020) Development of poly (ethylene oxide) bioactive nanocomposite films functionalized with zein nanoparticles. Coll Surf A Physicochem Eng Asp 586:124268
39. Gurusiddappa J, Madhuri W, Suvarna RP, Dasan KP (2016) Studies on the morphology and conductivity of PEO/LiClO4. Materials Today Proceed 3(6):1451–1459

40. Akkaya A, Şahin B, Aydın R, Çetin H, Ayyıldız E (2020) Solution-processed nanostructured ZnO/CuO composite films and improvement its physical properties by lustrous transition metal silver doping. J Mater Sci Mater Electron 31(17):14400–14410
41. Miccoli I, Edler F, Pfnür H, Tegenkamp C (2015) The 100th anniversary of the four-point probe technique: the role of probe geometries in isotropic and anisotropic systems. J Phys Condens Matter 27(22):223201
42. Sengwa RJ, Choudhary S (2017) Dielectric and electrical properties of PEO-Al2O3 nanocomposites. J Alloys Compd 701:652–659
43. Morsi M, El-Khodary SA, Rajeh A (2018) Enhancement of the optical, thermal and electrical properties of PEO/PAM: Li polymer electrolyte films doped with Ag nanoparticles. Physica B 539:88–96
44. Pillai P, Khurana P, Tripathi A (1986) Dielectric studies of poly (methyl methacrylate)/polystyrene double layer system. J Mater Sci Lett 5(6):629–632
45. Mohamad A et al (2003) Ionic conductivity studies of poly (vinyl alcohol) alkaline solid polymer electrolyte and its use in nickel–zinc cells. Solid State Ionics 156(1–2):171–177
46. Elashmawi I, Abdelrazek E, Ragab H, Hakeem NJPBCM (2010) Structural, optical and dielectric behavior of PVDF films filled with different concentrations of iodine. Phys B Condens Matter 405(1):94–98
47. Cultrera A et al (2019) Mapping the conductivity of graphene with electrical resistance tomography. Sci Rep 9(1):1–9

Authors and Affiliations

A. B. Migdadi[1] · Ahmad A. Ahmad[1] · Ahmad M. Alsaad[1] · Qais M. Al-Bataineh[3] · Ahmad Telfah[2,3]

[1] Department of Physical Sciences, Jordan University of Science & Technology, P.O. Box 3030, Irbid 22110, Jordan

[2] Hamdi Mango Center for Scientific Research, (HMCSR), Jordan University, Amman 11942, Jordan

[3] Leibniz Institut für Analytische Wissenschaften-ISAS-e.V., Bunsen-Kirchhoff-Straße 11, 44139 Dortmund, Germany